2014

STM Study of Pulsed Laser Assisted Growth of Ge Quantum Dot on Si(1 0 0)-(2 × 1)

Ali Orguz Er
Old Dominion University

Hani E. Elsayed-Ali
Old Dominion University, helsayed@odu.edu

Regular Article

STM study of pulsed laser assisted growth of Ge quantum dot on Si(1 0 0)-(2 × 1)

Ali Oguz Er[1] and Hani E. Elsayed-Ali[2,a]

[1] Department of Physics, Old Dominion University, Norfolk, 23529 VA, USA
[2] Department of Electrical and Computer Engineering and the Applied Research Center, Old Dominion University, Norfolk, 23529 VA, USA

Abstract. Ge quantum dot formation on Si(1 0 0)-(2 × 1) by nanosecond pulsed laser deposition under laser excitation was investigated. Scanning tunneling microscopy was used to probe the growth mode and morphology. Excitation was performed during deposition using laser energy density of 25–100 mJ/cm^2. Faceted islands were achieved at a substrate temperature of ~250 °C only when using laser excitation. The island morphology changes with increased laser excitation energy density although the faceting of the individual islands remains the same. The size of the major length of islands increases with the excitation laser energy density. A purely electronic mechanism of enhanced surface diffusion of the Ge adatoms is proposed.

1 Introduction

The growth of Ge quantum dots (QD) on silicon has attracted much attention due to Ge/Si QD applications in nanoelectronics and optoelectronic devices and the importance of this system in understanding heteroepitaxy [1]. Once the wetting layer is completed, the film grows as three-dimensional islands in order to relieve lattice strain. Some of the islands could be dislocation free but can develop misfit dislocations as their size grows due to strain [2]. In vapor-phase deposition, as the growth proceeds beyond the wetting layer, hut-shaped faceted islands develop. These are rectangular-shaped 105-faceted islands having a contact angle ∼ 11° with {1 0 0} planes [2]. With the increase in Ge coverage, multifaceted, dome-shape islands are observed to coexist with huts [3]. While the {1 0 5}-faceted huts have a 15–20 nm average size, the domes are mainly bound by steeper facets, such as {1 1 3} and {1 0 2}, making ∼ 25° and 26° with {1 0 0} planes, respectively, and have an average size of 50–100 nm [4].

The morphological evolution of Ge islands is dependent on growth conditions [5]. Generally, increasing the substrate temperature above that needed for epitaxial growth at a certain coverage causes an increase in island size and height, a decrease in the number of islands, and their shape transition from hut to dome [6].

Low temperature thin film growth is important in microelectronic fabrication in order to avoid interdiffusion, which degrades the interface properties in multilayers.

In Ge/Si, one way to suppress misfit dislocations is to lower the growth temperature [7]. Pulsed ion-beam irradiation during heteroepitaxy of Ge on Si led to modifying the average size and size distribution of Ge islands grown by molecular beam epitaxy (MBE) and post-deposition nanosecond pulsed laser treatment of Ge QD grown on Si reduced the QD surface density, modified their composition and increased their average size, making the QD size more uniform after the treatment [8].

We have studied the effects of pulsed laser induced electronic excitations on the self-assembly of Ge QD on Si(1 0 0)-(2 × 1) grown by pulsed laser deposition (PLD) [9,10]. Here we expand the scope of our previous observations with reflection high-energy electron diffraction (RHEED) by conducting an ultrahigh vacuum scanning tunneling microscopy (STM) study of the laser excitation effect on deposition at different laser energy densities. The effect of applying the excitation laser on the growth morphology is studied. The results are consistent with an electronically driven mechanism that increases surface diffusion of the Ge adatoms.

2 Experiment

Germanium quantum dots were grown in an ultrahigh vacuum (UHV) chamber (∼ 7×10^{-11} Torr) by PLD equipped with STM. The Ge target was rotated at 6 rpm to minimize particle formation during deposition. The laser beam profile on target and target rotation speed were set such

[a] e-mail: helsayed@odu.edu

that the spatial separation of the laser pulse spots on target were ~0.6 of its full width at half-maximum (FWHM), resulting in ablation of the target surface by no more than two laser pulses. The Si(1 0 0) substrates (dimensions of 1.0 mm × 10 mm × 0.5 mm, p-type boron doped, resistivity 0.060–0.075 Ω cm, and miscut angle 0.38°) were chemically etched by using a modified Shiraki method before being loaded into the UHV chamber. The Ge target was a 2″ diameter disk, 0.5 mm thick, undoped n-type, with a resistivity of 45.0–58.7 Ω cm. After loading the target and substrate, the vacuum chamber was pumped down, baked for more than 24 h, and finally left to cool down to room temperature. The Si(1 0 0) substrate was degassed overnight at ~ 700 °C and then flashed to ~ 1200 °C for ~60 s to obtain the (2 × 1) reconstruction. The substrate was heated by direct current. The surface temperature was measured using a Mikron MI-GA15 pyrometer.

A Q-switched Nd:YAG (wavelength λ = 1064 nm, FWHM of ~40 ns, 10-Hz repetition rate) was split into an ablation beam and an excitation beam of nonequal powers by means of a half-wave plate and a thin film polarizing beam splitter. The p-polarized ablation beam was focused on the rotating Ge target to a spot size ~400 μm (measured at $1/e$ of the peak value), resulting in a laser energy density of ~8 J/cm^2. This resulted in a deposition rate of ~1.6 × 10^{-3} ML/pulse (~0.0016 ML/s), as determined from STM observation and confirmed by ex situ measurement by spectroscopic ellipsometry. The s-polarized excitation beam was left unfocused with a beam diameter of ~6.0 mm (measured at $1/e$ peak value) and was used to irradiate the sample surface. Both the ablation and the excitation laser beams were incident on the Ge target and Si substrate at 45°.

## 3 Results and discussions

Ge deposition was conducted on a clean, reconstructed Si(1 0 0)-(2 × 1). Figure 1 shows STM image of a 10 × 10 nm^2 area on the Si(1 0 0)-(2 × 1) surface which reveals two kinds of steps and various kinds of defects. These local structures play an important role in semiconductor processing. The surface shows a step that has a mixed S$_A$ (smooth) and S$_B$ (ragged) character with dimer rows on upper and lower terraces and dimers rotated 90° relative to each other on consecutive terraces.

Figure 2 shows two- and three-dimensional STM images obtained over an area 500 × 500 nm^2 after ~6 ML Ge growth on Si(1 0 0) at 250 °C. The three-dimensional (3D) structures are multifaceted dome-like islands and have a wide distribution of sizes. Our previous RHEED results showed that for PLD at similar laser ablation conditions and Ge coverage, the Ge film does not grow epitaxially at a substrate temperature of 250 °C if the deposition is performed without electronic excitation of the substrate [9,11]. The RHEED pattern of the Si(1 0 0)-(2 × 1) substrate at 250 °C was very similar to that at room temperature with exception of the small reduction in diffraction intensity due to the Debye-Waller factor.
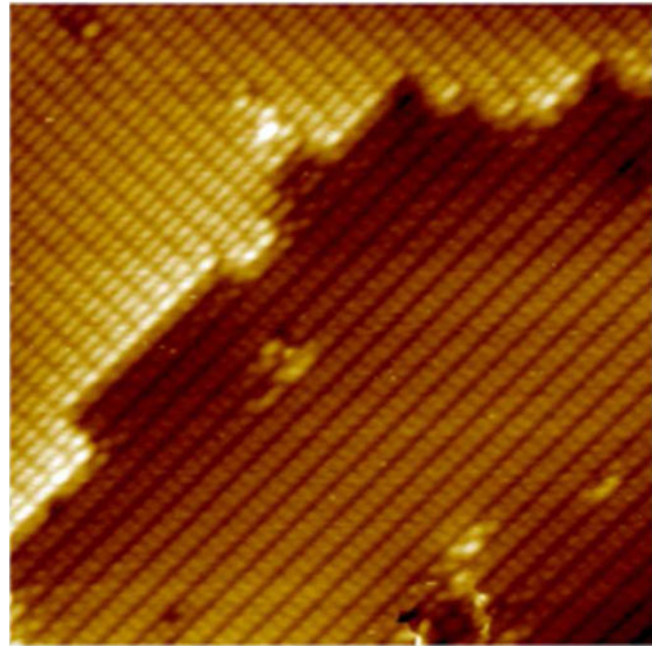
Fig. 1. STM image of clean Si(1 0 0)-(2 × 1) surface acquired over 10 × 10 nm^2 area.
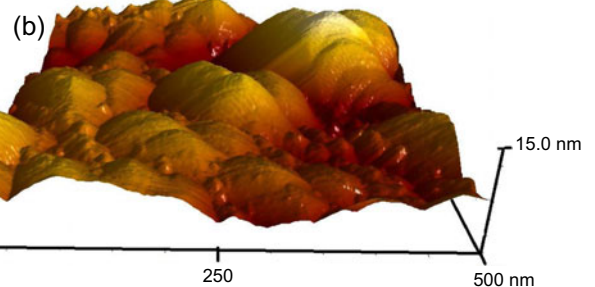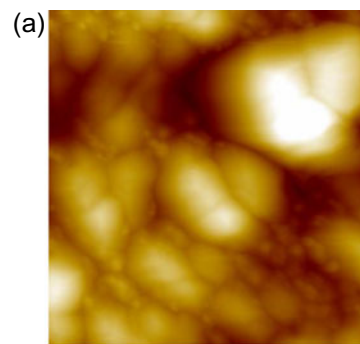
Fig. 2. STM image over 500 × 500 nm^2 area deposited at 250 °C. (a) Two-dimensional image; (b) three dimensional image.

The growth was then repeated also with the substrate temperature at 250 °C but with applying excitation laser energy pulses with different laser energy densities. The effect of surface excitation on growth morphology was studied. In Figure 3, the excitation laser-energy density of 75 mJ/cm^2 was used. The excitation laser energy density varied over the surface by ~10% due to the spatial variation in the laser beam profile and pulse-to-pulse
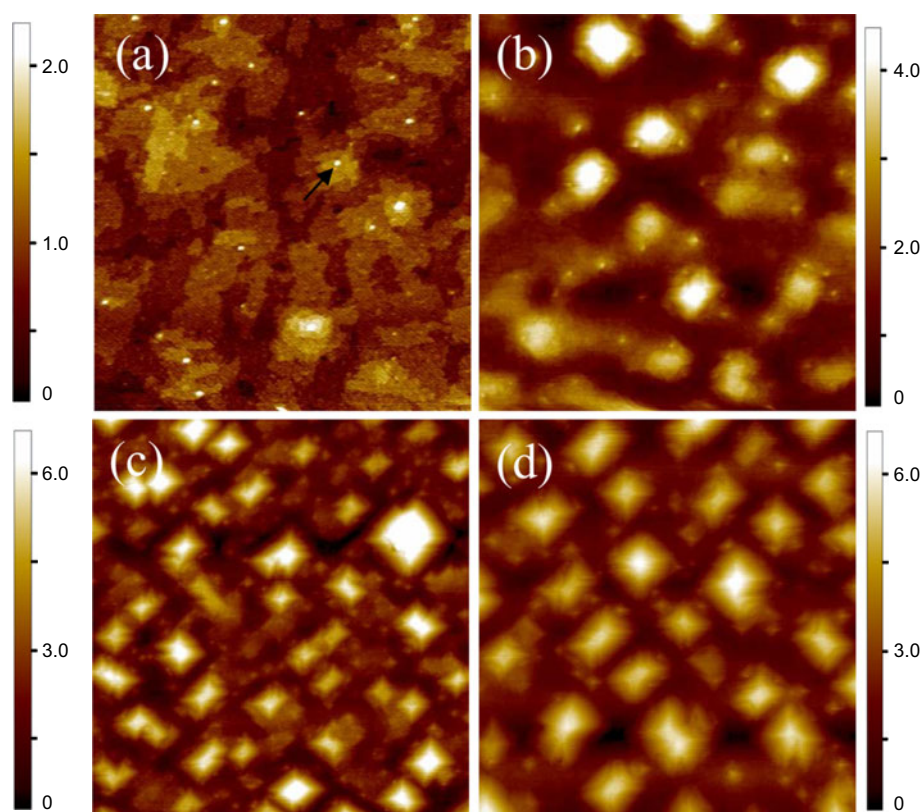
Fig. 3. Ge coverage on Si(1 0 0) at (a) 2 ML, (b) 4 ML, (c) 5 ML and (d) 6 ML when 75 mJ/cm^2 excitation laser energy density was used. (All images are 500 × 500 nm^2). Deposition was performed at 250 °C. STM observation conducted at room temperature. The color scale bar at the side of each image represents the height in nm. The arrow in (a) points to a Ge cluster on top of a wetting layer 2D patch.

fluctuations. Growth formation was studied at different Ge coverages. At 2 ML, flat patches of the Ge wetting layer are observed with a few Ge clusters grown on top of the wetting layer, as shown in Figure 3a. As the coverage was increased to ∼4 ML, 3D islands started to appear, as shown in Figure 3b. At this coverage, the faceting of islands is mainly {1 0 5} with the Si(1 0 0) plane. Figure 3c, obtained at 5 ML coverage, shows {1 0 5}-faceted pyramidal-shaped islands along with square-based islands. When the Ge coverage reaches ∼6 ML, the islands maintain the same morphology while their average island major length increases, as shown in Figure 3d. The STM image obtained at 6 ML shows islands well distributed over the surface area and with similar shapes and sizes. Three distinctive island shapes are observed. These are rectangular-based huts, square-based pyramids and some multifaceted domes. The majority of these islands are square-based pyramidal with a fraction of huts and domes. The faceted shape of islands is indicative of the crystalline growth at this condition. Figure 4 shows the size distribution of islands obtained at 6 ML coverage and shows that the average island major length is ∼68 nm while the most expected length is 70 nm. The full width at half-maximum (FWHM) of the size distribution is 21 nm. The coverage ratio is ∼36%, and island density is 3.0×10^{10} island/cm^2.
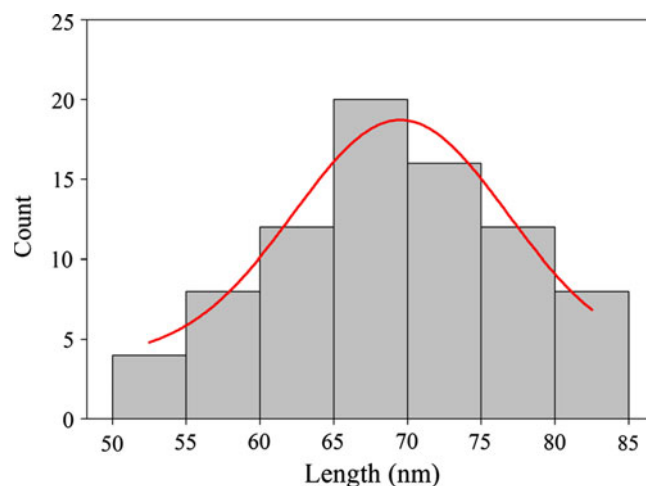
Fig. 4. The size distribution of the major length of islands for 6 ML Ge coverage. The excitation laser energy density is 75 mJ/cm^2 while ablation laser energy density is 8 J/cm^2. Deposition was performed at 250 °C. STM observation conducted at room temperature.

Figure 5 shows the characteristic individual island at ∼6 ML Ge coverage at different excitation laser energy densities. Figure 5a shows predominantly rectangular-based huts when 25 mJ/cm^2 excitation laser energy
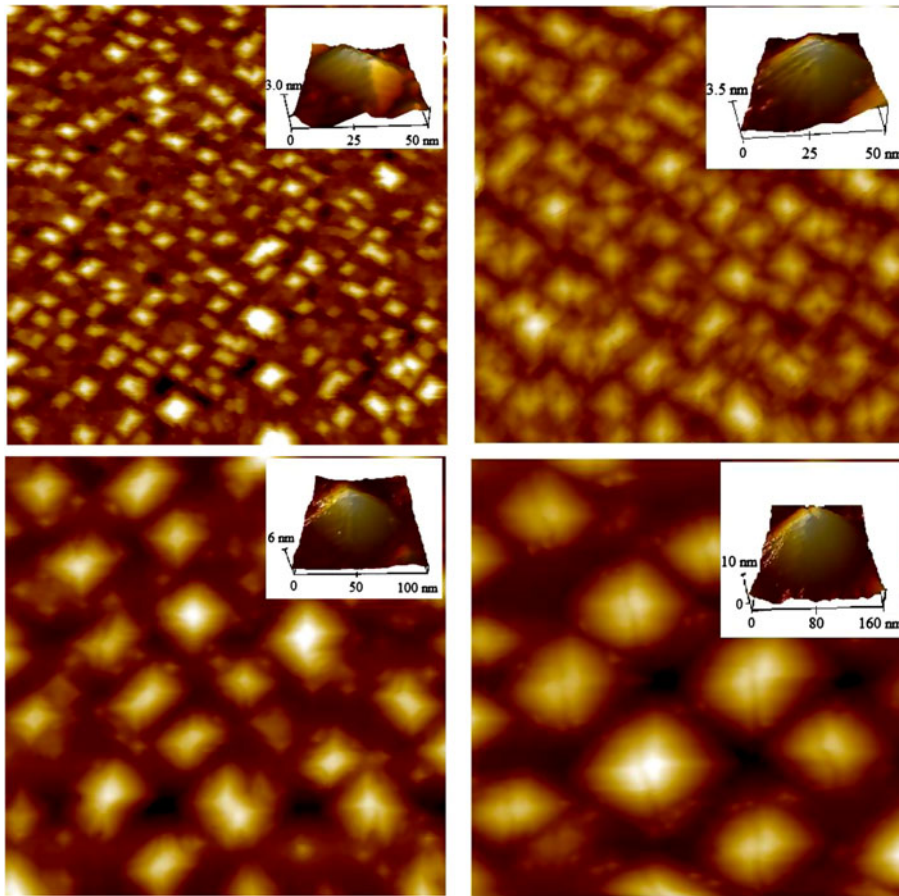
Fig. 5. STM image of Ge islands inside over an area of 500×500 nm^2 when laser energy densities of (a) 25 mJ/cm^2, (b) 50 mJ/cm^2, (c) 75 mJ/cm^2 and (d) 100 mJ/cm^2 are used for excitation. The inset shows the predominant shape of islands.

density was used. When the excitation is increased to 50 mJ/cm^2, it was observed that the average island's size increases, as shown in Figure 5b. This trend continues when the laser energy density is increased to 75 mJ/cm^2, as shown in Figure 5c. It was observed that the lateral aspect ratio, defined as minor length/major length, is decreasing when excitation energy is increased [11]. Finally, Figure 5d shows characteristic island shape obtained when 100 mJ/cm^2 excitation laser is used. In this case, domes are observed to be the dominant shape, with island size relatively larger compared to other films. As can be seen from Figure 6, the average island major length increases with the excitation laser energy density.

The rectangular-based huts and square-based pyramids transform into dome-shaped islands while the average length, height and area increase with the increase of the excitation laser energy density from 25 to 100 mJ/cm^2. Although the morphology of the final films changes with the excitation laser energy density, the faceting planes of the individual islands do not change. When the lowest laser energy density is used, most of the islands consisted of pyramidal-shaped islands, mainly {1 0 5}-faceted islands with different shapes and sizes. When 25 mJ/cm^2 excitation laser energy density is used and after $\sim$6 ML deposition, we generally observed small size ($\leq$40 nm)
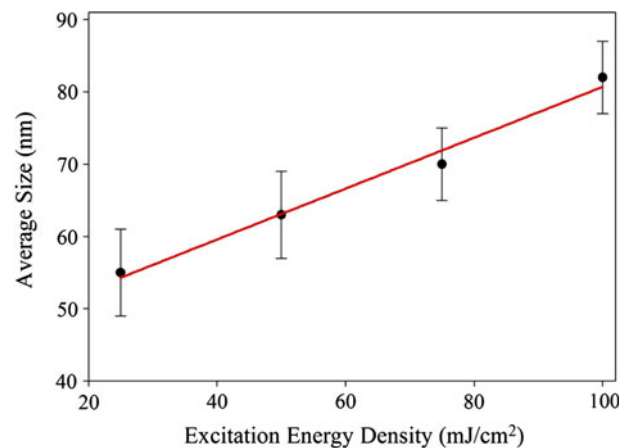
Fig. 6. The dependence of the size the major length of islands on the excitation laser energy density. Deposition was performed at 250 °C, while STM observation was conducted at room temperature.

square-based islands, while at larger laser energy densities, rectangular-based islands also appeared with same faceting. When 100 mJ/cm^2 is used, the faceting basically remained the same, while the size and height increased, as it can be seen in Figure 5d.

When the surface is irradiated by the pulsed laser, the initial effect is to generate electron-hole pairs. Bulk silicon has an indirect bandgap of 1.12 eV. The primary effect of the 1064 nm (1.17 eV) nanosecond laser light on the Si substrate is bulk-valence excitation to generate holes and electrons with small excess energies. The energy density of the ns laser pulses used is well below the melting threshold of Si.

The surface temperature rise due to laser heating was calculated by using a one-dimensional heat-diffusion model. The maximum temperature rise due to absorption of the 1064 nm excitation laser in the skin depth of Si ($\sim 60~\mu$m) was found to be ~ 23 °C at 100 mJ/cm^2 excitation energy density. The surface temperature drops to the substrate temperature by heat diffusion in $\sim 0.1~\mu$s. For Ge, the skin depth for 1064 nm is ~ 200 nm, and the maximum temperature rise in this case is ~ 200 °C if irradiated with 100 mJ/cm^2, which is the maximum laser energy density used during the present work.

The results show that irradiation of the substrate by the excitation laser has an effect on Ge growth similar to that observed when the substrate temperature is raised. Basically, there appears to be a mechanism driven by the excitation laser that results in enhanced Ge adatom surface diffusion. The macroscopic diffusion of Ge atoms adsorbed on the Si(1 0 0)-(2 × 1) surface has been shown to follow the Arrhenius behavior [12]: $D = D_0 \exp[-E_T/kT]$, where $D_o = 4.3 \times 10^{-4}$ cm^2/s is a pre-exponential constant, $E_T = 1.17$ eV is the activation energy and k and T are the Boltzmann's constant and temperature, respectively. The Ge atoms move just $\sim 1.6 \times 10^{-11}$ cm in 100 ns at 250 °C, which is clearly too small to affect the nucleation and growth mechanism. Therefore, the temperature rise due to laser heating could be excluded as a possible mechanism affecting Ge growth morphology due to the short temperature excursion time and small temperature rise.

An electron or a photon interacting with the surface can induce an electronic excitation. Emission of ions or neutral particles due to this excitation can occur. Such processes are referred to as desorption induced by electronic transitions (DIET). Two established DIET mechanisms are the Knotek-Feibelman (KF) model and the Menzel, Gomer and Redhead (MGR) model [13–15]. However, due to small photon energy in the present study, which is only ~ 0.05 eV above the Si bandgap, the electronic transition probability for DIET will be too small to cause any desorption or significant vibrational excitation at the Si surface.

The two-hole localization (THL) model was proposed and applied successfully to explain electronically induced bond rupture at Si and other surfaces [16]. This model assumes that surface bond rupture, leading to neutral-atomic desorption, can be induced by strong lattice relaxations associated with localization of two valence holes on the same surface bond. The localization of the second hole causes strong vibrations of the surface atom, which could lead to bond breaking. Atoms could be ejected due to this transient strong lattice vibration (phonon kick) with a distribution of translational energies that starts from

a given onset [17]. Vibrational relaxation after electronic excitation would lead to many phonons being emitted. The lattice forms a continuum of motions that can absorb the energy of the vibrational relaxation. As the energy of the surface atoms increases, the bonded atoms vibrate more strongly. If the phonon kick perpendicular to the surface imparted to a surface atom is not sufficient to cause desorption, the enhanced vibrational motion could lead to increased surface diffusion.

A possible scenario involves electron-hole generation in the substrate followed by hole diffusion to the surface and two-hole localization [16]. The laser-induced desorption of Si adatoms on Si(1 0 0)-(2 × 1) when the surface is excited by 1064 nm, 3.5 ns laser pulses was investigated [18]. Their results show that electronic excitation causes desorption of Si atoms from a certain adatom configuration. The desorption yield was super-linearly dependent on the laser fluence and, therefore, was consistent with the THL model. The results show that free holes are more effectively trapped at surface-defect sites. This suggests that substrate excitation during deposition causes hole localization preferentially at adatom sites. For laser irradiation with a fluence of 12 mJ cm^{-2}, the total vacancy generation density was $\sim 2.5 \times 10^{-3}$ ML after 1000 pulses and $\sim 5.6 \times 10^{-3}$ ML after 10 000 pulses, showing saturation in vacancy density generation with laser pulses as was also predicted theoretically [18]. In the present study, the laser pulse was split into two; one used for ablation while the other for excitation. Thin film growth and laser excitation were occurring simultaneously. The deposition rate was $\sim 1.6 \times 10^{-3}$ ML/pulse, which is much higher than any expected vacancy production per pulse. Therefore, vacancy production by laser irradiation is expected to have negligible contribution to the growth morphology. It is the excitation-induced increase in the surface diffusion of adatoms that affects the growth. Moreover, heating Si(1 0 0)-(2 × 1) to 250 °C does not affect its surface structure except for the small increase in surface atom mean vibrational amplitude due to the Debye-Waller factor. For clean Si(1 0 0) surface, the (2 × 1) reconstruction is stable up to 930±20 K at which a structural phase transition starts to occur [19].

Once the Ge wetting layer is formed, THL can occur on the Ge surface. At 250 °C, the indirect Ge energy bandgap is 0.57 eV and Ge has a direct bandgap at 0.7 eV. The absorption coefficient of 1064 nm in Ge is 1.6×10^4 cm^{-1}, leading to significantly higher electron-hole generation in the Ge wetting layer than the Si substrate. The hole density in Ge due to absorption of the 100 mJ/cm^2, 1064 nm laser pulse is $\sim 10^{23}$ cm^{-3}. The surface hole density depends on many parameters that include surface recombination and diffusion across the Ge/Si interface. We are not aware of any study done on electronic bond breaking on electronically excited Ge surfaces. However, the THL mechanism, followed by the phonon-kick, is applicable to semiconductors in general. It is energetically possible that this mechanism could be effective on Ge surfaces. The phonon-kick has to transfer enough energy to the top atom along the bond direction to break that bond. When energy transfer is not sufficient for bond breaking, then the atom

will have a vibrational excitation that can lead to surface hopping. Therefore, THL on the Ge surface can lead to selective energy transfer to the Ge adatoms since these atoms constitute a defect site. The energy that is preferentially given to these adsorbed atoms can result in their hopping to settle epitaxially on the surface. Measurement of Ge film thickness for different excitation laser energy densities showed that the Ge coverage is not affected by the excitation laser; thus, we conclude that atom desorption by electronic excitation is too small for the studied conditions.

Charge transfer from the substrate to the adsorbate can cause surface atoms to gain vibrational energy [20]. Charge transfer interactions are believed to be important and can occur at the interface of an Si substrate [21]. Photoinduced charge transfer between the Ge atoms and Si substrate or the Ge wetting layer may affect the nucleation by increasing the vibrational energy of surface atoms, causing an increase in the surface diffusion. The low photon energy used in the present study, with only ~0.05 eV excess energy above the Si bandgap at 300 K, makes this process unlikely for Si surface. Although charge transfer is more effective in organic semiconductors [22], we cannot completely rule out a possible role of charge transfer between the Ge surface and the Ge adatoms.

In Ge/Si growth, the deposition rate plays an important role in the size, density and uniformity of Ge QD [23]. Low growth rates could also affect the purity of Ge clusters [23]. In our case, the transition from non-epitaxial to epitaxial growth was achieved by laser excitation of the substrate with all other conditions, including the deposition rate (PLD coverage per pulse and pulse rate) kept constant.

4 Summary

We have studied the effect of nanosecond pulsed laser excitation on the self-assembly of Ge quantum dots grown by pulsed laser deposition on Si(1 0 0)-(2 × 1) by STM. The morphology, growth temperature and the facet behavior of Ge quantum dots were studied at different excitation laser energy densities. The formation of {1 0 5}-faceted pyramids was observed right after the completion of the wetting layer. No effect on faceting was observed due to excitation laser energy. The electronic excitation during growth was found to (1) improve the quantum dot crystalline quality as observed by facet development, (2) change their morphology and (3) reduce epitaxial growth temperature. We propose a purely electronic mechanism of enhanced surface diffusion of the Ge adatoms.

References

1. K.L. Wang, C. Dongho, L. Jianlin, C. Chen, Proc. IEEE **95**, 1866 (2007)
2. D.J. Eaglesham, M. Cerullo, Phys. Rev. Lett. **64**, 1943 (1990)
3. M. Tomitori, K. Watanabe, M. Kobayashi, O. Nishikawa, Appl. Surf. Sci. **76–77**, 322 (1994)
4. F.M. Ross, R.M. Tromp, M.C. Reuter, Science **286**, 1931 (1999)
5. G. Capellini, M. De Seta, F. Evangelisti, Mat. Sci. Eng. B **89**, 184 (2002)
6. G. Jin, J.L. Liu, K.L. Wang, Appl. Phys. Lett. **83**, 2847 (2003)
7. W. Ensinger, Nucl. Instrum. Methods Phys. Res. B **127–128**, 796 (1997)
8. V. Volodin, A. Yakimov, A. Dvurechenskiǐ, M. Efremov, A. Nikiforov, E. Gatskevich, G. Ivlev, G. Mikhalev, Semiconductors **40**, 202 (2006)
9. M.S. Hegazy, H.E. Elsayed-Ali, J. Appl. Phys. **104**, 124302 (2008)
10. A.O. Er, H.E. Elsayed-Ali, Appl. Surf. Sci. **257**, 8078 (2011)
11. A.O. Er, H.E. Elsayed-Ali, J. Appl. Phys. **109**, 084320 (2011)
12. D. Srivastava, B.J. Garrison, Phys. Rev. B **46**, 1472 (1992)
13. M.L. Knotek, P.J. Feibelman, Phys. Rev. Lett. **40**, 964 (1978)
14. D. Menzel, R. Gomer, J. Chem. Phys. **41**, 3311 (1964)
15. P.A. Redhead, Can. J. Phys. **42**, 886 (1964)
16. H. Sumi, Surf. Sci. **248**, 382 (1991)
17. J. Kanasaki, K. Iwata, K. Tanimura, Phys. Rev. Lett. **82**, 644 (1999)
18. E. Inami, K. Tanimura, Phys. Rev. B **76**, 035311 (2007)
19. J.S. Ha, E.F. Greene, J. Chem. Phys. **91**, 571 (1989)
20. N.M. Hwang, D.Y. Kim, Int. Mater. Rev. **49**, 171 (2004)
21. R. Ruiz, D. Choudhary, B. Nickel, T. Toccoli, K.-C. Chang, A.C. Mayer, P. Clancy, J.M. Blakely, R.L. Headrick, S. Iannotta, G.G. Malliaras, Chem. Mater. **16**, 4497 (2004)
22. B. Park, P. Paoprasert, I. In, J. Zwickey, P.E. Colavita, R.J. Hamers, P. Gopalan, P.G. Evans, Adv. Mat. **19**, 4353 (2007)
23. Y. Zhang, M. Floyd, K.P. Driver, J. Drucker, P.A. Crozier, D.J. Smith, Appl. Phys. Lett. **80**, 3623 (2002)